

Improved constraint on Higgs boson self-couplings with quartic and cubic power dependence in the cross section

Hai Tao Li¹, Zong-Guo Si¹, Jian Wang^{1,2}, Xiao Zhang¹, Dan Zhao¹

¹*School of Physics, Shandong University, Jinan, Shandong 250100, China*

²*Center for High Energy Physics, Peking University, Beijing 100871, China*

Abstract

Precise information on the Higgs boson self-couplings provides the foundation for unveiling the electroweak symmetry breaking mechanism. Due to the scarcity of Higgs boson pair events at the LHC, only loose limits have been obtained. This is based on the assumption that the cross section is a quadratic function of the trilinear Higgs self-coupling in the κ framework. However, if higher-order corrections of virtual Higgs bosons are included, the function form would dramatically change. In particular, new quartic and cubic power dependence on the trilinear Higgs self-coupling would appear. To get this new function form, we have performed a specialized renormalization procedure suitable for tracking all the Higgs self-couplings in each calculation step. Moreover, we introduce renormalization of the scaling parameter in the κ framework to ensure the cancellation of all ultraviolet divergences. With the new function forms of the cross sections in both the gluon-gluon fusion and vector boson fusion channels, the upper limit of $\kappa_{\lambda_3} = \lambda_{3H}/\lambda_{3H}^{\text{SM}}$ by the ATLAS (CMS) collaboration is reduced from 6.6 (6.49) to 5.4 (5.37). However, it is still hard to extract a meaningful constraint on the quartic Higgs self-coupling λ_{4H} from Higgs boson pair production data. We also present the invariant mass distributions of the Higgs boson pair at different values of κ_{λ} , which could help to set optimal cuts in the experimental analysis.

1 Introduction

After the discovery of the Higgs boson at the Large Hadron Collider (LHC) [1, 2], precise measurements of its properties, such as the mass, spin, and couplings to gauge bosons and fermions, have become critically important [3–9]. To date, these measurements have been consistent with the expectations of the Standard Model (SM) [10, 11]. However, the trilinear and quartic Higgs self-couplings, i.e., λ_{3H} and λ_{4H} , which play special roles in the spontaneous electroweak (EW) symmetry breaking, stability of the universe [12] and precision test of the SM, are still subject to large uncertainties.

A lot of efforts have been devoted to improving the measurement of the Higgs self-coupling. The most direct approach involves measuring the cross section of Higgs boson pair production. The dominant channel is the production via gluon-gluon fusion (ggF). At the leading order (LO), the process occurs via a top-quark loop. In the large m_t limit, using so called Higgs effective field theory, the cross section of ggF Higgs boson pair production is known up to next-to-next-to-next-to-leading-order (N³LO) QCD corrections [13–17]. The soft gluon resummation effect was also calculated [18–20]. With full top quark mass dependence, only next-to-leading-order (NLO) QCD correction is currently available [21–24]. Estimates of the top-quark mass effects at next-to-next-to-leading-order (NNLO) have been performed by [25–29]. To provide an accurate simulation of the events, a fully differential calculation of the Higgs boson pair production and decay to the $b\bar{b}\gamma\gamma$ final state with exact top quark mass at QCD NLO was presented [30]. In addition, the NLO EW corrections have been investigated in [31–37]. The subdominant channel—vector boson fusion (VBF)—has also been calculated up to N³LO in QCD [38–41].

Using the data of Higgs boson pair production at the Run 2 LHC, the current best constraints are $-0.6 < \kappa_{\lambda_{3H}} < 6.6$ [42] and $-1.24 < \kappa_{\lambda_{3H}} < 6.49$ [11] extracted from the ATLAS and CMS measurements, respectively, in the κ framework, in which $\kappa_{\lambda_{3H}} = \lambda_{3H}/\lambda_{3H}^{\text{SM}}$ with λ_{3H}^{SM} being the SM value of the trilinear Higgs self-coupling. On the one hand, the process of single Higgs boson production and decay depends on the Higgs self-coupling via higher-order EW corrections and can also provide certain constraint [43–48]. A measurement performed by CMS using the differential fiducial cross section in bins of p_T^H sets the constraint as $-5.4 < \kappa_{\lambda_{3H}} < 14.9$ [49]. A combined analysis of the single Higgs and double Higgs data by ATLAS shows that the constraint on the Higgs self-coupling is $-0.4 < \kappa_{\lambda_{3H}} < 6.3$ at 95% confidence level with the assumption that the new physics changes only the Higgs self-coupling [42].

The above constraints are obtained based on the fact that the cross section of Higgs boson pair production can be taken as a function of the Higgs self-couplings. Indeed, even with higher-order QCD corrections, the cross section is a quadratic function of the trilinear Higgs self-coupling λ_{3H} . Nevertheless, higher-order EW corrections incorporate contributions from Feynman diagrams containing one or more triple Higgs or quadruple Higgs vertices. These corrections exhibit a distinct functional dependence on the Higgs self-coupling. Specifically, new quartic and cubic dependence on the trilinear Higgs self-coupling would appear, which has a significant impact on the constraints given that the present upper limit is so large.

However, in practice, it is not obvious to keep the explicit dependence on the Higgs self-coupling, which is considered a derived parameter in the conventional calculation of EW corrections, especially in the renormalization procedure; see, e.g., Refs. [35, 50]. In the SM, the Higgs boson self-coupling λ is determined by the Higgs boson mass and the vacuum expectation value. Therefore, the calculation in the SM can not be simply extended to the case with general λ_{3H} and λ_{4H} , and the result with higher power (beyond quadratic) dependence on the Higgs self-couplings in the general κ framework is still unavailable. In this work, we propose a renormalization procedure that explicitly keeps the Higgs self-couplings, and calculate the cross sections of the Higgs boson pair production via both ggF and VBF. Our results show that the upper limit of $\kappa_{\lambda_{3H}}$, which is 6.6 by ATLAS (6.49 by CMS), can be reduced by about 20% after including higher power dependence of the cross section on the Higgs self-couplings.

2 Renormalization in the κ framework

The LO contribution to the ggF Higgs boson pair production $g(p_1)g(p_2) \rightarrow H(p_3)H(p_4)$ comes from the top-quark induced triangle and box Feynman diagrams, which are of order λ_{3H} and λ_{3H}^0 , respectively. Consequently, the LO cross section at the 13 TeV LHC is given by

$$\sigma_{\text{ggF,LO}}^{\kappa_\lambda} = (4.72 \kappa_{\lambda_{3H}}^2 - 23.0 \kappa_{\lambda_{3H}} + 35.0) \text{ fb.} \quad (1)$$

The subscript λ_{3H} in $\kappa_{\lambda_{3H}}$ indicates that this factor measures the deviation of the trilinear Higgs coupling. Below we will also need $\kappa_{\lambda_{4H}}$ to represent the modification of the quartic Higgs self-coupling. The SM cross section is reproduced at $\kappa_{\lambda_{3H}} = 1$ and $\kappa_{\lambda_{4H}} = 1$. The quadratic function form persists even if higher-order QCD corrections are included [51], e.g.,

$$\sigma_{\text{ggF,NNLO-FT}}^{\kappa_\lambda} = (10.8 \kappa_{\lambda_{3H}}^2 - 49.6 \kappa_{\lambda_{3H}} + 70.0) \text{ fb,} \quad (2)$$

where the full one-loop real contributions are combined with the other NNLO QCD corrections in the large m_t limit. Compared with Eq. (1), the QCD corrections are so significant that each term in $\kappa_{\lambda_{3H}}$ has more than doubled.

The EW corrections would change the above function form in two aspects. First, the coefficients of the quadratic, linear, and constant terms would be changed. However, the magnitude is only a few percent as indicated by the calculation in Ref. [35]. This kind of correction marginally affects the constraints on Higgs self-coupling and thus is neglected in our study. Second, higher power or new dependence on the Higgs self-couplings arises. One can see in Fig. 1 some typical two-loop Feynman diagrams, which would make contributions of order λ_{3H}^3 , λ_{3H}^2 , $\lambda_{4H}\lambda_{3H}$, λ_{4H} to the amplitudes. As a result, the cross section would then contain the quartic and cubic λ_{3H} terms and start to be sensitive to the quartic Higgs self-coupling λ_{4H} . It is the purpose of our work to investigate these corrections, which are labeled by $\delta\sigma_{\text{EW}}^{\kappa_\lambda}$ below, and their impact on the constraints for the Higgs self-couplings.

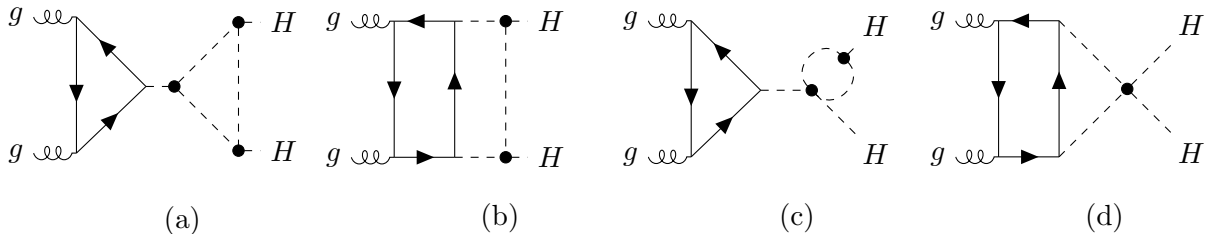


Figure 1: Typical two-loop Feynman diagrams of order λ_{3H}^3 (a), λ_{3H}^2 (b), $\lambda_{4H}\lambda_{3H}$ (c) and λ_{4H} (d), respectively.

Our calculation of the two-loop diagrams proceeds as follows. We use **FEYNARTS** [52] to generate the Feynman diagrams and amplitudes. The amplitudes are written as a linear combination of two tensor structures with the coefficients called form factors. After performing the Dirac algebra with **FEYNCALC** [53–55], we are left with scalar integrals for each form factor. We did not attempt to reduce all of them to master integrals and construct the differential equations for the master integrals as in conventional methods. Instead, we chose to calculate the scalar integrals directly with the numerical package **AMFLOW** [56, 57] for specific phase space points. The main reason is that the construction of the differential equation is time-consuming with general kinematic dependence. Even if the differential equation is obtained, the analytical solution seems not feasible with current technologies. Numerical solutions of the differential equations often suffer from accuracy loss. Direct numerical calculation at each phase space point ensures accuracy. The challenge lies in covering the entire phase space efficiently. Fortunately, the process of $gg \rightarrow HH$ is dominated by the S-wave component, rendering the amplitude insensitive to the scattering angle. Moreover, its dependence on the scattering energy is also

weak, except in very high-energy regions, as illustrated below. These characteristics allow us to generate a grid with a limited data set, which can be used to accurately calculate the amplitude at any point in the phase space.

Notice that the sum of all one-particle irreducible two-loop diagrams is finite. But the one-particle reducible two-loop diagrams contain ultraviolet divergences. They will cancel after considering the contributions from the counter-terms in renormalization.

In the SM, the Lagrangian for the Higgs sector can be written as

$$\mathcal{L}_H = (D_\mu \phi_0)^\dagger (D^\mu \phi_0) + \mu_0^2 (\phi_0^\dagger \phi_0) - \lambda_0 (\phi_0^\dagger \phi_0)^2, \quad (3)$$

where ϕ_0 denotes the bare Higgs doublet and D_μ is the covariant derivative. The relations between the bare fields and couplings, and their renormalized counterparts, are given by $\phi_0 = Z_\phi^{1/2} \phi$, $\mu_0^2 = Z_{\mu^2} \mu^2$, and $\lambda_0 = Z_\lambda \lambda$.

The EW gauge symmetry is spontaneously broken once the Higgs field develops a non-vanishing vacuum expectation value v . Taking the unitary gauge, we write the Higgs field as

$$\phi = \frac{1}{\sqrt{2}} \begin{pmatrix} 0 \\ H + Z_v v \end{pmatrix}, \quad (4)$$

where Z_v is the renormalization constant for the vacuum expectation value. The renormalized Lagrangian in the κ framework after EW gauge symmetry breaking is written as

$$\begin{aligned} \mathcal{L}_H = & \frac{1}{2} Z_\phi (\partial_\mu H)^2 - \left(-\frac{1}{2} Z_{\mu^2} Z_\phi Z_v^2 \mu^2 v^2 + \frac{1}{4} Z_\lambda Z_\phi^2 Z_v^4 \lambda v^4 \right) - (Z_\lambda Z_\phi^2 Z_v^3 \lambda v^3 - Z_{\mu^2} Z_\phi Z_v \mu^2 v) H \\ & - \left(\frac{3}{2} Z_\lambda Z_\phi^2 Z_v^2 \lambda v^2 - \frac{1}{2} Z_{\mu^2} Z_\phi \mu^2 \right) H^2 - Z_{\kappa_{3H}} Z_\lambda Z_\phi^2 Z_v \lambda_{3H} v H^3 - \frac{1}{4} Z_{\kappa_{4H}} Z_\lambda Z_\phi^2 \lambda_{4H} H^4 + \dots, \end{aligned} \quad (5)$$

where the ellipsis represents the terms involving EW gauge bosons. Note that the letter λ is solely used for the Higgs self-coupling in the SM but $\lambda_{3H} \equiv \kappa_{\lambda_3} \lambda$ and $\lambda_{4H} \equiv \kappa_{\lambda_4} \lambda$ denote the Higgs self-couplings that could be modified by new physics. We have added renormalization constants $Z_{\kappa_{3H}}$ and $Z_{\kappa_{4H}}$ for the rescaling parameters κ_{λ_3} and κ_{λ_4} to account for potential new physics effect in renormalization. Following the general principle of the κ framework, we have assumed that the new physics does not affect the vacuum expectation value and Higgs mass when we rescale the Higgs self-couplings. The second term in the first line does not contain any field and thus can be safely dropped. Writing $Z = 1 + \delta Z$, the third term can be expanded as

$$(\mu^2 v - \lambda v^3) H + [(\delta Z_{\mu^2} + \delta Z_\phi + \delta Z_v) \mu^2 v - (\delta Z_\lambda + 2\delta Z_\phi + 3\delta Z_v) \lambda v^3] H + \dots \quad (6)$$

where we have neglected higher-order corrections that are products of two δZ . We choose the renormalization condition such that there is no tadpole contribution. This condition requires $\mu^2 = \lambda v^2$ at the tree level, and $(\delta Z_{\mu^2} - \delta Z_\lambda - \delta Z_\phi - 2\delta Z_v) \mu^2 v + T = 0$ at the one-loop level with T being the contribution from the one-loop tadpole diagrams. δZ_v would be determined after considering the renormalization of the EW gauge sector. Since we focus on the corrections induced by the Higgs self-coupling, we can simply take $\delta Z_v + \delta Z_\phi/2 = 0$. We adopt dimensional regularization, i.e., setting the space-time dimension $d = 4 - 2\epsilon$, to symbolize the ultraviolet divergence and take μ_R as the renormalization scale. The tadpole diagram is evaluated to be

$$T = \frac{3\lambda_{3H} v}{16\pi^2} m_H^2 \left(\frac{1}{\epsilon} + \ln \frac{\mu_R^2}{m_H^2} + 1 \right). \quad (7)$$

The mass m_H of the Higgs boson can be determined from the quadratic term in Eq. (5),

$$\frac{1}{2} (\partial_\mu H)^2 - \mu^2 H^2 - \left(\frac{3}{2} \delta Z_\lambda + \frac{5}{2} \delta Z_\phi - \frac{1}{2} \delta Z_{\mu^2} + 3\delta Z_v \right) \mu^2 H^2$$

$$\equiv \frac{1}{2}(\partial_\mu H)^2 - \frac{1}{2}m_H^2 H^2 + \frac{1}{2}\delta Z_\phi(\partial_\mu H)^2 - \frac{1}{2}(\delta Z_{m_H^2} + \delta Z_\phi)m_H^2 H^2. \quad (8)$$

On the right-hand side, we have introduced the classical mass terms. By comparing both sides, it is straightforward to get $m_H^2 = 2\mu^2$ and $\delta Z_{m_H^2} \equiv \frac{3}{2}\delta Z_\lambda + \frac{3}{2}\delta Z_\phi - \frac{1}{2}\delta Z_{\mu^2} + 3\delta Z_v$. We choose the on-shell renormalization condition for the Higgs field and obtain

$$\begin{aligned} \delta Z_{m_H^2} &= \frac{3\lambda_{4H}}{16\pi^2} \left(\frac{1}{\epsilon} + \ln \frac{\mu_R^2}{m_H^2} + 1 \right) + \frac{9\lambda_{3H}^2 v^2}{m_H^2} \frac{1}{8\pi^2} \left(\frac{1}{\epsilon} + \ln \frac{\mu_R^2}{m_H^2} + 2 - \frac{\pi}{\sqrt{3}} \right), \\ \delta Z_\phi &= \frac{9\lambda_{3H}^2 v^2}{8\pi^2} \frac{\sqrt{3} - 2\pi/3}{\sqrt{3}m_H^2}. \end{aligned} \quad (9)$$

Combining the above equations, we derive the results for the other renormalization constants, δZ_{μ^2} and δZ_λ . Then the counter-term for the triple Higgs interaction in Eq. (5) is given by

$$\begin{aligned} \delta\lambda_{3H} &\equiv \delta Z_\lambda + 2\delta Z_\phi + \delta Z_v + \delta Z_{\kappa_{3H}} \\ &= -\frac{3\lambda_{3H}}{16\pi^2} \left(\frac{1}{\epsilon} + \ln \frac{\mu_R^2}{m_H^2} + 1 \right) + \frac{3\lambda_{4H}}{16\pi^2} \left(\frac{1}{\epsilon} + \ln \frac{\mu_R^2}{m_H^2} + 1 \right) \\ &\quad + \frac{3\lambda_{3H}^2 v^2}{16\pi^2 m_H^2} \left(\frac{6}{\epsilon} + 6 \ln \frac{\mu_R^2}{m_H^2} + 21 - 4\sqrt{3}\pi \right) + \delta Z_{\kappa_{3H}} \end{aligned} \quad (10)$$

with $\delta Z_{\kappa_{3H}} \equiv Z_{\kappa_{3H}} - 1$.

Including the contribution of counter-terms, we obtain the result with explicit Higgs self-coupling dependence for the one-particle reducible diagrams,

$$\begin{aligned} \mathcal{M}_{gg \rightarrow H^* \rightarrow HH}^{\text{LO}} &\times \left\{ \frac{3}{16\pi^2} \frac{1}{\epsilon} \left(-2\lambda_{4H} - \lambda_{3H} + 6\lambda_{3H}^2 \frac{v^2}{m_H^2} \right) + \delta Z_{\kappa_{3H}} \right. \\ &+ \frac{3}{16\pi^2} \ln \frac{\mu_R^2}{m_H^2} \left[-2\lambda_{4H} - \lambda_{3H} + 6\lambda_{3H}^2 \frac{v^2}{m_H^2} \right] \\ &- \frac{9\lambda_{3H}^2}{8\pi^2} \frac{v^2}{s - m_H^2} \left[\beta \left(\ln \left(\frac{1 - \beta}{1 + \beta} \right) + i\pi \right) + \frac{s}{m_H^2} \left(1 - \frac{2\pi}{3\sqrt{3}} \right) + \frac{5\pi}{3\sqrt{3}} - 1 \right] \\ &+ \frac{3\lambda_{3H}^2}{16\pi^2} \frac{v^2}{m_H^2} (21 - 4\sqrt{3}\pi) - \frac{9\lambda_{3H}^2 v^2}{4\pi^2} C_0[m_H^2, m_H^2, s, m_H^2, m_H^2, m_H^2] \\ &\left. - \frac{3\lambda_{4H}}{16\pi^2} \left[\beta \left(\ln \left(\frac{1 - \beta}{1 + \beta} \right) + i\pi \right) + 5 - \frac{2\pi}{\sqrt{3}} \right] - \frac{3\lambda_{3H}}{16\pi^2} \right\}, \end{aligned} \quad (11)$$

where $s = (p_1 + p_2)^2$, $\beta = \sqrt{1 - 4m_H^2/s}$ and $C_0[m_H^2, m_H^2, s, m_H^2, m_H^2, m_H^2]$ is a scalar integral that can be calculated by Package-X [58]. $\mathcal{M}_{gg \rightarrow H^* \rightarrow HH}^{\text{LO}}$ is the LO amplitude which contains the Higgs self-coupling. In the SM, the divergences in the first line vanish and $\delta Z_{\kappa_{3H}}$ is not needed. In the general κ framework, it is essential to include $\delta Z_{\kappa_{3H}}$ in renormalization. We adopt the $\overline{\text{MS}}$ scheme to subtract the divergences. As a result, the rescaling parameter is scale-dependent. If it is expressed in terms of the value at the scale m_H , then an additional contribution from its perturbative expansion cancels the above $\ln(\mu_R^2/m_H^2)$ term exactly.

Now it is ready to compute the finite part of the squared amplitudes. We set the two-dimensional grid as a function of the Higgs velocity β and $\cos\theta$ with θ the scattering angle. The range of β is from 0 to 1, and $\cos\theta$ is also taken from 0 to 1 since the squared amplitudes are symmetric under $\theta \rightarrow \pi - \theta$. The grids for the LO squared amplitudes and λ dependent EW corrections are illustrated in Fig. 2. We see that the squared amplitudes are stable against the change within the region $\beta < 0.6$. For larger β , the LO amplitudes rise dramatically and then start to drop when $\beta > 0.9$. In contrast, the λ dependent correction first decreases and then increases when β is larger than 0.85. These variations are mainly due

to the large logarithms $\ln^i(1 - \beta)$. And therefore we have constructed the grid as a function of $\ln^i(1 - \beta)$ for $\beta \geq 0.96$. We have tested the grid by comparing the generated values¹ and the ones obtained by direct high-precision computation for the LO squared amplitude at some phase space points that are not on the grid lattice. We find good agreement at the per-mille level. We have used the grid to calculate the total cross section by performing the convolution with the parton distribution function (PDF) and phase space integrations. Comparing it to the result obtained using analytical expressions or the OPENLOOPS package [59–61], we find that the relative difference is lower than $\mathcal{O}(10^{-3})$.

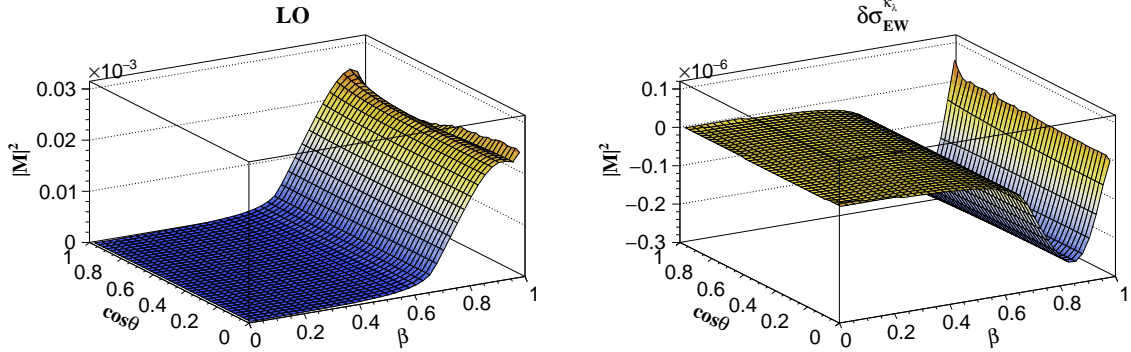


Figure 2: The squared matrix elements of LO and λ dependent EW corrections.

The LO cross section of the VBF channel also exhibits a quadratic dependence on the trilinear Higgs coupling. The higher power dependence can be obtained by calculating the one-loop diagrams with an additional Higgs propagator. The calculation is standard except for the renormalization, which has been illustrated above. We have implemented our analytical results in the PROVBFHH program [41, 62] and used the QCDLOOP package [63] to evaluate the scalar one-loop integrals.

3 Numerical results and updated constraints on Higgs boson self-coupling

In our numerical calculations, we take $v = (\sqrt{2} G_F)^{-1/2}$ with the Fermi constant $G_F = 1.16637 \times 10^{-5} \text{ GeV}^{-2}$, the Higgs boson mass $m_H = 125 \text{ GeV}$, and the top quark mass $m_t = 173 \text{ GeV}$. For the VBF channel, we set the EW gauge boson masses $M_W = 80.379 \text{ GeV}$ and $M_Z = 91.1876 \text{ GeV}$. We use the PDF4LHC15_nlo_100_pdfas PDF set [64], and the associating strong coupling α_s . The default renormalization scale in α_s and the factorization scale in the PDF are chosen to be $\mu_{R,F} = m_{HH}/2$ in the ggF channel and $\mu_{R,F} = \sqrt{-q_i^2}$ in the VBF channel with m_{HH} being the Higgs pair invariant mass and q_i being the transferred momenta from fermion lines.

The EW corrections that contain higher power dependence on the Higgs self-coupling are given by

$$\delta\sigma_{\text{ggF,EW}}^{\kappa_\lambda} = (0.075\kappa_{\lambda_3}^4 - 0.158\kappa_{\lambda_3}^3 - 0.006\kappa_{\lambda_3}^2\kappa_{\lambda_4} - 0.058\kappa_{\lambda_3}^2 + 0.070\kappa_{\lambda_3}\kappa_{\lambda_4} - 0.149\kappa_{\lambda_4}) \text{ fb}$$

for the ggF channel and

$$\begin{aligned} \delta\sigma_{\text{VBF,EW}}^{\kappa_\lambda} = & (0.0215\kappa_{\lambda_3}^4 - 0.0324\kappa_{\lambda_3}^3 - 0.0019\kappa_{\lambda_3}^2\kappa_{\lambda_4} - 0.0043\kappa_{\lambda_3}^2 \\ & + 0.0151\kappa_{\lambda_3}\kappa_{\lambda_4} - 0.0211\kappa_{\lambda_4}) \text{ fb} \end{aligned} \quad (12)$$

¹The Lagrange interpolation method is used to generate the squared amplitudes at the phase space point not on the lattice.

for the VBF channel. We have computed all the $\mathcal{O}(\lambda_{3H}^i)$, $i \geq 2$ contributions in the amplitude. The above $\kappa_{\lambda_3}^2$ terms arise because we want to keep the cancellation relation between the $\mathcal{O}(\lambda_{3H})$ and $\mathcal{O}(1)$ amplitudes at LO. The cubic $\kappa_{\lambda_3}^3$ and quartic $\kappa_{\lambda_3}^4$ terms appear for the first time up to this perturbative order. Though their coefficients are rather small, they provide notable corrections to the cross section if κ_{λ_3} is chosen much larger than 1. As seen from table 1, the λ dependent corrections in the ggF (VBF) channel reach 91% (82%) of the LO cross section for $\kappa_{\lambda_3} = 6$.

κ_{λ_3}	κ_{λ_4}	ggF			VBF		
		$\sigma_{\text{LO}}^{\kappa_{\lambda}}$	$\sigma_{\text{NNLO-FT}}^{\kappa_{\lambda}}$	$\delta\sigma_{\text{EW}}^{\kappa_{\lambda}}$	$\sigma_{\text{LO}}^{\kappa_{\lambda}}$	$\sigma_{\text{NNNLO}}^{\kappa_{\lambda}}$	$\delta\sigma_{\text{EW}}^{\kappa_{\lambda}}$
1	1	16.7	31.2	-0.225	1.71	1.69	-2.30×10^{-2}
3	1	8.59	18.4	1.28	3.59	3.53	8.35×10^{-1}
6	1	67.3	161	60.6	25.1	24.6	20.7
1	3	16.7	31.2	-0.393	1.71	1.69	-3.89×10^{-2}
1	6	16.7	31.2	-0.646	1.71	1.69	-6.27×10^{-2}
3	3	8.59	18.4	1.30	3.59	3.53	8.50×10^{-1}
6	6	67.3	161	61.0	25.1	24.6	20.7

Table 1: Cross sections (in fb) of ggF and VBF Higgs boson pair production for different κ_{λ_3} and κ_{λ_4} at the 13 TeV LHC.

In addition, there is a new dependence on the quartic Higgs self-coupling λ_{4H} . Because this dependence is only linear and the corresponding coefficients are small, their contributions are negligible. From table 1, it can be observed that the cross section varies by 0.6% when κ_{λ_4} changes from 1 to 6 while keeping $\kappa_{\lambda_3} = 6$. As a consequence, we do not expect that a meaningful constraint on the quartic Higgs self-coupling can be extracted from Higgs pair production at the 13 TeV LHC.

We can make a comparison with the results in Refs. [31, 65]. The authors of these papers have obtained similar expressions for the cross sections in the ggF channel. However, they have assumed that the triple and quartic Higgs self-couplings are modified by one dimension-six and one dimension-eight operators. They performed calculations, especially renormalization, in terms of the coefficients of higher-dimensional operators, and then transformed the results onto the basis of κ_{λ_3} and κ_{λ_4} . These results can not be directly compared with the experimental analysis in the κ framework.

In figure 3, we show different perturbative predictions for the cross section of Higgs boson pair production at the 13 TeV LHC as a function of $\kappa_{\lambda_3} = \kappa_{\lambda_4} = \kappa_{\lambda}$. It is obvious that higher-order perturbative corrections dramatically change the function form. The current experimental upper limit by the ATLAS (CMS) collaborations on κ_{λ} is 6.6 (6.49) based on the theoretical calculations at QCD NNLO in the ggF channel and NNNLO in the VBF channel; see table 1. Taking $\delta\sigma_{\text{EW}}^{\kappa_{\lambda}}$ corrections into account and assuming that the QCD and EW corrections are factorizable, the upper limit is narrowed down to 5.4 (5.37). These limits are almost the same when keeping $\kappa_{\lambda_4} = 1$. If the scale uncertainties are considered [66], the upper limit spans in the range (6.5, 6.8) in the ATLAS result, which would decrease to (5.4, 5.6) after including higher power dependence. In the CMS result, the upper limit changes from (6.40, 6.67) to (5.31, 5.48). The lower limits are only modified slightly.

Lastly, the Higgs boson pair invariant mass distributions in the ggF channel are shown in figure 4. The peak position moves from 400 GeV to 260 GeV when κ_{λ} changes from 1 to 6, which indicates the Higgs bosons tend to be produced with very small velocity in the case of

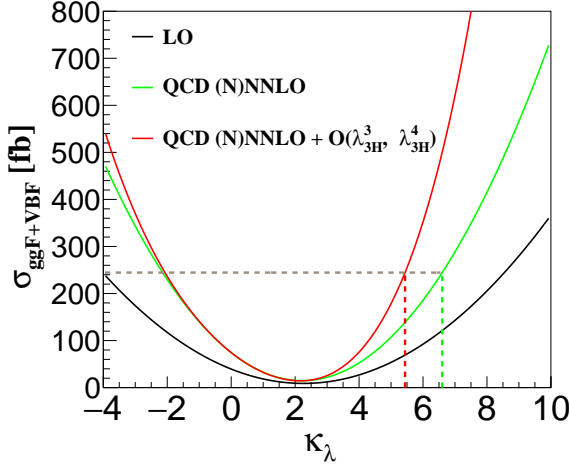


Figure 3: Cross sections of Higgs boson pair production as a function of $\kappa_{\lambda_3} = \kappa_{\lambda_4} = \kappa_\lambda$ at the 13 TeV LHC including both ggF and VBF processes. The black line represents the LO result, and the green line denotes the result with (N)NNLO QCD corrections in the ggF (VBF) channel. The red line indicates the result with higher power dependence on the Higgs boson self-coupling.

large κ_λ values. For $\kappa_\lambda = 3$, there is a bump around $m_{HH} = 450$ GeV. These features may help to set optimal cuts in the experimental analysis. From this figure, we also observe that the λ dependent corrections have a great impact on the distributions, especially in the small m_{HH} region, and therefore they should be included in future studies.

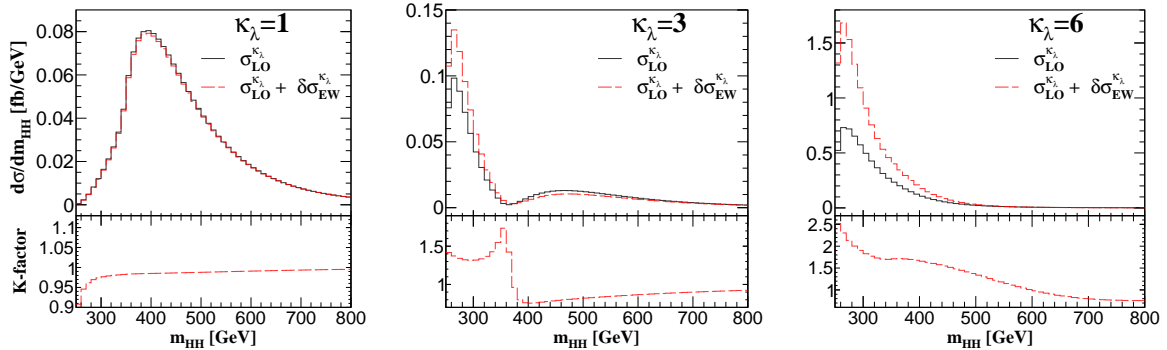


Figure 4: The distributions of Higgs boson pair invariant mass at LO and with $\delta\sigma_{\text{EW}}^{\kappa_\lambda}$ corrections at the 13 TeV LHC. We have used $\kappa_{\lambda_3} = \kappa_{\lambda_4} = \kappa_\lambda$.

4 Conclusion

The exact shape of the Higgs potential is one of the most important mysteries in particle physics. The current limits on the Higgs self-coupling are predominantly derived based on the assumption that the cross section of the Higgs boson pair production is a quadratic function of the self-coupling. We find that the function form should be generalized to include quartic and cubic dependence on the self-coupling which arise due to higher-order corrections induced by virtual Higgs bosons.

We adopt a proper renormalization procedure to keep track of all the contributions from Higgs self-couplings. The complicated two-loop squared amplitudes are computed numerically

and a grid is generated for the calculation of the cross section. We present numerical contributions of the quartic and cubic terms of the trilinear Higgs self-coupling in the cross section at the LHC. With this refined functional form, we demonstrate that the upper limit on the trilinear Higgs self-coupling normalized by the SM value is reduced from 6.6 (by ATLAS) and 6.49 (by CMS) to 5.4 and 5.37, respectively. This improvement is achieved without more data being analyzed, highlighting the importance of including higher power dependence on the Higgs self-coupling in the cross section.

Moreover, we find it hard to obtain any useful constraint on the quartic Higgs self-coupling from Higgs boson pair production. One may resort to triple Higgs boson production. This requires a collider with higher energies than the LHC. In the future, it would also be interesting to investigate the impact of even higher power dependence to see if the limit could be strengthened further.

Acknowledgments

We would like to thank Huan-Yu Bi, Yan-Qing Ma, and Huai-Min Yu for comparing their numerical results of the two-loop amplitudes. We also thank Shan Jin, Yefan Wang and Lei Zhang for helpful discussion. This work was supported in part by the National Science Foundation of China under grant No. 12275156, No. 12321005, No. 12375076 and the Taishan Scholar Foundation of Shandong province (tsqn201909011).

References

- [1] ATLAS collaboration, G. Aad et al., *Observation of a new particle in the search for the Standard Model Higgs boson with the ATLAS detector at the LHC*, *Phys. Lett. B* **716** (2012) 1–29, [[1207.7214](#)].
- [2] CMS collaboration, S. Chatrchyan et al., *Observation of a New Boson at a Mass of 125 GeV with the CMS Experiment at the LHC*, *Phys. Lett. B* **716** (2012) 30–61, [[1207.7235](#)].
- [3] CMS collaboration, A. M. Sirunyan et al., *A measurement of the Higgs boson mass in the diphoton decay channel*, *Phys. Lett. B* **805** (2020) 135425, [[2002.06398](#)].
- [4] ATLAS collaboration, G. Aad et al., *Measurement of the Higgs boson mass in the $H \rightarrow ZZ^* \rightarrow 4\ell$ decay channel using 139 fb^{-1} of $\sqrt{s} = 13\text{ TeV}$ pp collisions recorded by the ATLAS detector at the LHC*, *Phys. Lett. B* **843** (2023) 137880, [[2207.00320](#)].
- [5] CMS collaboration, A. Tumasyan et al., *Measurement of the Higgs boson width and evidence of its off-shell contributions to ZZ production*, *Nature Phys.* **18** (2022) 1329–1334, [[2202.06923](#)].
- [6] ATLAS collaboration, G. Aad et al., *Study of the spin and parity of the Higgs boson in diboson decays with the ATLAS detector*, *Eur. Phys. J. C* **75** (2015) 476, [[1506.05669](#)].
- [7] CMS collaboration, V. Khachatryan et al., *Constraints on the spin-parity and anomalous HVV couplings of the Higgs boson in proton collisions at 7 and 8 TeV*, *Phys. Rev. D* **92** (2015) 012004, [[1411.3441](#)].
- [8] CMS collaboration, A. Tumasyan et al., *Measurements of the Higgs boson production cross section and couplings in the W boson pair decay channel in proton-proton collisions at $\sqrt{s} = 13\text{ TeV}$* , *Eur. Phys. J. C* **83** (2023) 667, [[2206.09466](#)].

[9] ATLAS collaboration, G. Aad et al., *Determination of the relative sign of the Higgs boson couplings to W and Z bosons using WH production via vector-boson fusion with the ATLAS detector*, 2402.00426.

[10] ATLAS collaboration, G. Aad et al., *A detailed map of Higgs boson interactions by the ATLAS experiment ten years after the discovery*, *Nature* **607** (2022) 52–59, [2207.00092].

[11] CMS collaboration, A. Tumasyan et al., *A portrait of the Higgs boson by the CMS experiment ten years after the discovery*, *Nature* **607** (2022) 60–68, [2207.00043].

[12] G. Degrassi, S. Di Vita, J. Elias-Miro, J. R. Espinosa, G. F. Giudice, G. Isidori et al., *Higgs mass and vacuum stability in the Standard Model at NNLO*, *JHEP* **08** (2012) 098, [1205.6497].

[13] S. Dawson, S. Dittmaier and M. Spira, *Neutral Higgs boson pair production at hadron colliders: QCD corrections*, *Phys. Rev. D* **58** (1998) 115012, [hep-ph/9805244].

[14] D. de Florian and J. Mazzitelli, *Higgs Boson Pair Production at Next-to-Next-to-Leading Order in QCD*, *Phys. Rev. Lett.* **111** (2013) 201801, [1309.6594].

[15] D. de Florian, M. Grazzini, C. Hanga, S. Kallweit, J. M. Lindert, P. Maierhöfer et al., *Differential Higgs Boson Pair Production at Next-to-Next-to-Leading Order in QCD*, *JHEP* **09** (2016) 151, [1606.09519].

[16] L.-B. Chen, H. T. Li, H.-S. Shao and J. Wang, *Higgs boson pair production via gluon fusion at N^3LO in QCD*, *Phys. Lett. B* **803** (2020) 135292, [1909.06808].

[17] L.-B. Chen, H. T. Li, H.-S. Shao and J. Wang, *The gluon-fusion production of Higgs boson pair: N^3LO QCD corrections and top-quark mass effects*, *JHEP* **03** (2020) 072, [1912.13001].

[18] D. Y. Shao, C. S. Li, H. T. Li and J. Wang, *Threshold resummation effects in Higgs boson pair production at the LHC*, *JHEP* **07** (2013) 169, [1301.1245].

[19] D. de Florian and J. Mazzitelli, *Higgs pair production at next-to-next-to-leading logarithmic accuracy at the LHC*, *JHEP* **09** (2015) 053, [1505.07122].

[20] A. H. Ajjath and H.-S. Shao, *N^3LO+N^3LL QCD improved Higgs pair cross sections*, *JHEP* **02** (2023) 067, [2209.03914].

[21] S. Borowka, N. Greiner, G. Heinrich, S. P. Jones, M. Kerner, J. Schlenk et al., *Higgs Boson Pair Production in Gluon Fusion at Next-to-Leading Order with Full Top-Quark Mass Dependence*, *Phys. Rev. Lett.* **117** (2016) 012001, [1604.06447].

[22] S. Borowka, N. Greiner, G. Heinrich, S. P. Jones, M. Kerner, J. Schlenk et al., *Full top quark mass dependence in Higgs boson pair production at NLO*, *JHEP* **10** (2016) 107, [1608.04798].

[23] J. Baglio, F. Campanario, S. Glaus, M. Mühlleitner, M. Spira and J. Streicher, *Gluon fusion into Higgs pairs at NLO QCD and the top mass scheme*, *Eur. Phys. J. C* **79** (2019) 459, [1811.05692].

[24] J. Baglio, F. Campanario, S. Glaus, M. Mühlleitner, J. Ronca, M. Spira et al., *Higgs-Pair Production via Gluon Fusion at Hadron Colliders: NLO QCD Corrections*, *JHEP* **04** (2020) 181, [2003.03227].

[25] M. Grazzini, G. Heinrich, S. Jones, S. Kallweit, M. Kerner, J. M. Lindert et al., *Higgs boson pair production at NNLO with top quark mass effects*, *JHEP* **05** (2018) 059, [1803.02463].

[26] M. L. Czakon and M. Niggetiedt, *Exact quark-mass dependence of the Higgs-gluon form factor at three loops in QCD*, *JHEP* **05** (2020) 149, [2001.03008].

[27] J. Mazzitelli, *NNLO study of top-quark mass renormalization scheme uncertainties in Higgs boson production*, *JHEP* **09** (2022) 065, [2206.14667].

[28] J. Davies, K. Schönwald and M. Steinhauser, *Towards $gg \rightarrow HH$ at next-to-next-to-leading order: Light-fermionic three-loop corrections*, *Phys. Lett. B* **845** (2023) 138146, [2307.04796].

[29] J. Davies, K. Schönwald, M. Steinhauser and M. Vitti, *Three-loop corrections to Higgs boson pair production: reducible contribution*, 2405.20372.

[30] H. T. Li, Z.-G. Si, J. Wang, X. Zhang and D. Zhao, *Higgs boson pair production and decay at NLO in QCD: the $b\bar{b}\gamma\gamma$ final state*, *JHEP* **04** (2024) 002, [2402.00401].

[31] S. Borowka, C. Duhr, F. Maltoni, D. Pagani, A. Shivaji and X. Zhao, *Probing the scalar potential via double Higgs boson production at hadron colliders*, *JHEP* **04** (2019) 016, [1811.12366].

[32] M. Mühlleitner, J. Schlenk and M. Spira, *Top-Yukawa-induced corrections to Higgs pair production*, *JHEP* **10** (2022) 185, [2207.02524].

[33] J. Davies, G. Mishima, K. Schönwald, M. Steinhauser and H. Zhang, *Higgs boson contribution to the leading two-loop Yukawa corrections to $gg \rightarrow HH$* , *JHEP* **08** (2022) 259, [2207.02587].

[34] J. Davies, K. Schönwald, M. Steinhauser and H. Zhang, *Next-to-leading order electroweak corrections to $gg \rightarrow HH$ and $gg \rightarrow gH$ in the large- m_t limit*, *JHEP* **10** (2023) 033, [2308.01355].

[35] H.-Y. Bi, L.-H. Huang, R.-J. Huang, Y.-Q. Ma and H.-M. Yu, *Electroweak Corrections to Double Higgs Production at the LHC*, *Phys. Rev. Lett.* **132** (2024) 231802, [2311.16963].

[36] G. Heinrich, S. Jones, M. Kerner, T. Stone and A. Vestner, *Electroweak corrections to Higgs boson pair production: The top-Yukawa and self-coupling contributions*, 2407.04653.

[37] J. Davies, K. Schönwald, M. Steinhauser and H. Zhang, *Electroweak corrections to $gg \rightarrow HH$: Factorizable contributions*, in *Loops and Legs in Quantum Field Theory*, 7, 2024, 2407.05787.

[38] R. Frederix, S. Frixione, V. Hirschi, F. Maltoni, O. Mattelaer, P. Torrielli et al., *Higgs pair production at the LHC with NLO and parton-shower effects*, *Phys. Lett. B* **732** (2014) 142–149, [1401.7340].

[39] L.-S. Ling, R.-Y. Zhang, W.-G. Ma, L. Guo, W.-H. Li and X.-Z. Li, *NNLO QCD corrections to Higgs pair production via vector boson fusion at hadron colliders*, *Phys. Rev. D* **89** (2014) 073001, [1401.7754].

[40] F. A. Dreyer and A. Karlberg, *Vector-Boson Fusion Higgs Pair Production at N^3LO* , *Phys. Rev. D* **98** (2018) 114016, [1811.07906].

[41] F. A. Dreyer and A. Karlberg, *Fully differential Vector-Boson Fusion Higgs Pair Production at Next-to-Next-to-Leading Order*, *Phys. Rev. D* **99** (2019) 074028, [1811.07918].

[42] ATLAS collaboration, G. Aad et al., *Constraints on the Higgs boson self-coupling from single- and double-Higgs production with the ATLAS detector using pp collisions at $s=13$ TeV*, *Phys. Lett. B* **843** (2023) 137745, [2211.01216].

[43] M. McCullough, *An Indirect Model-Dependent Probe of the Higgs Self-Coupling*, *Phys. Rev. D* **90** (2014) 015001, [1312.3322].

[44] M. Gorbahn and U. Haisch, *Indirect probes of the trilinear Higgs coupling: $gg \rightarrow h$ and $h \rightarrow \gamma\gamma$* , *JHEP* **10** (2016) 094, [1607.03773].

[45] G. Degrassi, P. P. Giardino, F. Maltoni and D. Pagani, *Probing the Higgs self coupling via single Higgs production at the LHC*, *JHEP* **12** (2016) 080, [1607.04251].

[46] W. Bizon, M. Gorbahn, U. Haisch and G. Zanderighi, *Constraints on the trilinear Higgs coupling from vector boson fusion and associated Higgs production at the LHC*, *JHEP* **07** (2017) 083, [1610.05771].

[47] S. Di Vita, C. Grojean, G. Panico, M. Riembau and T. Vantalon, *A global view on the Higgs self-coupling*, *JHEP* **09** (2017) 069, [1704.01953].

[48] J. Gao, X.-M. Shen, G. Wang, L. L. Yang and B. Zhou, *Probing the Higgs boson trilinear self-coupling through Higgs boson+jet production*, *Phys. Rev. D* **107** (2023) 115017, [2302.04160].

[49] CMS collaboration, A. Hayrapetyan et al., *Measurements of inclusive and differential cross sections for the Higgs boson production and decay to four-leptons in proton-proton collisions at $\sqrt{s} = 13$ TeV*, *JHEP* **08** (2023) 040, [2305.07532].

[50] A. Denner, *Techniques for calculation of electroweak radiative corrections at the one loop level and results for W physics at LEP-200*, *Fortsch. Phys.* **41** (1993) 307–420, [0709.1075].

[51] J. Alison et al., *Higgs boson potential at colliders: Status and perspectives*, *Rev. Phys.* **5** (2020) 100045, [1910.00012].

[52] T. Hahn, *Generating Feynman diagrams and amplitudes with FeynArts 3*, *Comput. Phys. Commun.* **140** (2001) 418–431, [hep-ph/0012260].

[53] R. Mertig, M. Bohm and A. Denner, *FEYN CALC: Computer algebraic calculation of Feynman amplitudes*, *Comput. Phys. Commun.* **64** (1991) 345–359.

[54] V. Shtabovenko, R. Mertig and F. Orellana, *New Developments in FeynCalc 9.0*, *Comput. Phys. Commun.* **207** (2016) 432–444, [1601.01167].

[55] V. Shtabovenko, R. Mertig and F. Orellana, *FeynCalc 9.3: New features and improvements*, *Comput. Phys. Commun.* **256** (2020) 107478, [2001.04407].

[56] X. Liu, Y.-Q. Ma and C.-Y. Wang, *A Systematic and Efficient Method to Compute Multi-loop Master Integrals*, *Phys. Lett. B* **779** (2018) 353–357, [1711.09572].

[57] X. Liu and Y.-Q. Ma, *AMFlow: A Mathematica package for Feynman integrals computation via auxiliary mass flow*, *Comput. Phys. Commun.* **283** (2023) 108565, [2201.11669].

[58] H. H. Patel, *Package-X 2.0: A Mathematica package for the analytic calculation of one-loop integrals*, *Comput. Phys. Commun.* **218** (2017) 66–70, [1612.00009].

[59] F. Caccioli, P. Maierhofer and S. Pozzorini, *Scattering Amplitudes with Open Loops*, *Phys. Rev. Lett.* **108** (2012) 111601, [1111.5206].

[60] F. Buccioni, S. Pozzorini and M. Zoller, *On-the-fly reduction of open loops*, *Eur. Phys. J. C* **78** (2018) 70, [1710.11452].

[61] OPENLOOPS 2 collaboration, F. Buccioni, J.-N. Lang, J. M. Lindert, P. Maierhöfer, S. Pozzorini, H. Zhang et al., *OpenLoops 2*, *Eur. Phys. J. C* **79** (2019) 866, [1907.13071].

[62] M. Cacciari, F. A. Dreyer, A. Karlberg, G. P. Salam and G. Zanderighi, *Fully Differential Vector-Boson-Fusion Higgs Production at Next-to-Next-to-Leading Order*, *Phys. Rev. Lett.* **115** (2015) 082002, [1506.02660].

[63] R. K. Ellis and G. Zanderighi, *Scalar one-loop integrals for QCD*, *JHEP* **02** (2008) 002, [0712.1851].

[64] J. Butterworth et al., *PDF4LHC recommendations for LHC Run II*, *J. Phys. G* **43** (2016) 023001, [1510.03865].

[65] W. Bizoń, U. Haisch and L. Rottoli, *Constraints on the quartic Higgs self-coupling from double-Higgs production at future hadron colliders*, *JHEP* **10** (2019) 267, [1810.04665].

[66] J. Baglio, F. Campanario, S. Glaus, M. Mühlleitner, J. Ronca and M. Spira, *gg → HH : Combined uncertainties*, *Phys. Rev. D* **103** (2021) 056002, [2008.11626].